Optimization of layer structure supporting long range surface plasmons for surface plasmon-enhanced fluorescence spectroscopy biosensors

Chun Jen Huang, Jakub Dostalek,[a] and Wolfgang Knoll
Austrian Institute of Technology, Tech Gate, Donau-City-Strasse 1, 1220 Vienna, Austria

(Received 10 September 2009; accepted 9 November 2009; published 7 January 2010)

Long range surface plasmons (LRSPs) are optical waves that propagate along thin metallic films with up to orders of magnitude lower damping compared to regular surface plasmons. Therefore, LRSPs attracted a great deal of attention for development of ultrasensitive biosensors based on surface plasmon resonance and surface plasmon-enhanced fluorescence spectroscopy (SPFS). In this article, the authors investigate the excitation of LRSPs on a biosensor-compatible layer structure consisting of a Cytop fluoropolymer, thin gold film modified by thiol self-assembled monolayer for coupling of receptor biomolecules, and an aqueous sample on its top. The morphology, and optical and electrical properties of the layer structure are determined and related to the performance of a SPFS biosensor. Through increasing the surface energy of Cytop fluoropolymer by O_2 plasma, more compact gold films that exhibit lower roughness were prepared which resulted in a higher binding capacity, decreased nonspecific adsorption of biomolecules to the biosensor surface, and in a larger enhancement of electromagnetic field intensity accompanied with the excitation of LRSPs. The authors show that by improving the quality of a gold film supporting LRSPs, the fluorescence signal can be enhanced up to sixfold with respect to regular SPFS biosensors. © *2010 American Vacuum Society.* [DOI: 10.1116/1.3271336]

I. INTRODUCTION

Surface plasmons (SPs) are optical waves that originate from collective oscillations of a charge density and the associated electromagnetic field at a metallic surface. On a thin metallic film embedded in dielectrics with similar refractive indices, SPs on the two opposite surfaces can couple through the film giving rise to a new surface plasmon mode referred to as long range surface plasmon (LRSP).[1] As this mode can propagate with orders of magnitude lower damping and its excitation are associated with narrower resonance compared to regular SPs; LRSPs attracted a great deal of attention in areas including integrated optical circuits,[2,3] nonlinear optics,[4–6] photoacoustics,[7] characterization of thin films,[8] and biosensors.[9–14] In biosensor applications, LRSPs are used to probe the binding of target molecules contained in an aqueous sample to biomolecular recognition sites anchored a metallic sensor surface. The spectroscopy of LRSP was employed for the measurement of refractive index changes induced by molecular binding.[10,12] Due to their lower damping, LRSPs allow the measurement of smaller refractive index variations[13] and thus provide more accurate detection of biomolecular binding events than the conventional surface plasmon resonance (SPR) sensors. In addition, LRSPs were employed in surface plasmon-enhanced fluorescence spectroscopy (SPFS) biosensors.[11,12] In this method, the binding of molecules labeled with a fluorophore is observed from changes in the intensity of fluorescence light emitted from the metallic sensor surface. SPFS takes advantage of the strong enhancement of the intensity of electromagnetic field upon the excitation of surface plasmons which directly increases the fluorescence signal from fluorophore-labeled molecules adhered to the surface.[15,16]

The majority of biosensors that exploit LRSPs rely on a layer structure consisting of a low refractive index buffer layer and a thin noble metal film (gold or silver). In these implementations, the refractive index of the buffer layer has to match to that of aqueous samples (close to 1.33 at the wavelength of $\lambda = 632.8$ nm) in order to achieve a symmetrical refractive index structure needed for the excitation of LRSPs. Up to date, fluoropolymers deposited by spincoating[10,14] or sputtering[17] and low refractive index dielectric layers such as aluminum fluoride[18] or magnesium fluoride[14] prepared by thermal evaporation were used for the construction of layer systems supporting LRSPs. In this contribution, we investigate thin gold films deposited on a Cytop fluoropolymer for the excitation of LRSPs on the surface of a SFPS biosensor. The characteristics of these films are related to the performance of this method by using a model experiment in which the affinity binding of protein molecules was observed through probing by LRSPs.

II. EXPERIMENT

A. Materials

Cytop fluoropolymer (CTL-809M, 9 wt % in the solvent of CT-solv 180) was obtained from Asahi Glass (Tokyo, Japan) and 99.99% Au grains were from Edelmetall (Neuss, Germany). 99.5% absolute ethanol, phosphate buffered saline (PBS), 95% triethylene glycol mono-11-mercaptoundecyl ether (PEG-thiol), Cy5-conjugated streptavidin (SA), and ethanolamine hydrochloride were purchased from Sigma-Aldrich (St. Louis, MO). *N*-hydroxysuccinimide

[a]Author to whom correspondence should be addressed; electronic mail: jakub.dostalek@ait.ac.at

(NHS) and 1-ethyl-3-(3-dimethylaminopropyl)carbodiimide (EDC) were acquired from Pierce (Rockford, IL). Biotin-terminated triethylene glycol mono-11-mercaptoundecyl ether (Biotin-thiol) was from ProChimia Surface (Sopot, Poland). Biotin-labeled polyclonal antibody (IgG) was from Acris Antibodies (Hiddenhausen, Germany). The Hellmanex II, LaSFN9 glass substrates ($76\times25\times1.5$ mm^3) were acquired from Hellma Optik (Jena, Germany). BK7 glass substrates ($76\times26\times1$ mm^3) were obtained from VWR (Wien, Austria).

B. Preparation of the layer structure

First, glass substrates were cleaned by sonicating in 2% Hellmanex II detergent for 20 min followed by extensive rinsing in H_2O and ethanol and drying under a stream of nitrogen. Cytop fluoropolymer was spin coated on a BK7 glass substrate, dried at room temperature for 1 h, and incubated at a temperature of $T=160$ °C for 1 h. The thickness of Cytop layers between 500 and 1300 nm was controlled by adjusting the rotation speed. In order to increase the surface energy of a Cytop film, its surface was exposed to O_2 plasma by using a Microwave plasma system 200 (PVA Tepla, Feldkirchen, Germany, microwave power of 100 W in an O_2 pressure of 20 mbars). After the O_2 etching, the substrates were stored in the laboratory atmosphere for at least 5 min in order to re-orientate the functionalities on the polymer surface, which resulted in a decrease in the surface energy by reaction with oxygen and water vapor in air.[19] Thin gold films were deposited on the top of Cytop surfaces by means of thermal evaporation (Edwards FL400, Boc Edwards, East Sussex, UK) with the evaporation rate of ~1.5 Å/s in a vacuum better than $\sim2.6\times10^{-6}$ mbar. After the gold deposition, the substrates were immediately soaked in a mixture of PEG and biotin terminated thiols (molar ratio 9:1) dissolved in absolute ethanol at a total concentration of 0.2 mM in order to form a self-assembled monolayer.[20] After overnight incubation, substrates were removed from the solution, rinsed with absolute ethanol, and dried in a stream of nitrogen.

C. Characterization of the layer structure

The surface morphology of the prepared layers was observed by using the MultiMode atomic force microscopy (AFM) (Veeco Instrumens, Santa Barbara, CA). Images were acquired in the tapping mode using a microcantilever (Olympus, Tokyo, Japan) with a spring constant of 42 N m^{-1} and resonance frequency of ~300 kHz. Thicknesses of thin films were determined by using a surface profiler (KLA-Tencor P-10). An ellipsometer EP^3-MW (Nanofilm Technologie GmbH, Germany) was used for the measurements of the refractive index of the thin Cytop films. The changes in surface energy were investigated at room temperature by using contact angle measurements and image processing software (DataPhysics Instruments, Filderstadt, Germany). The four-point collinear probe method was used for determining the resistivity of the gold layers deposited on top of Cytop. The

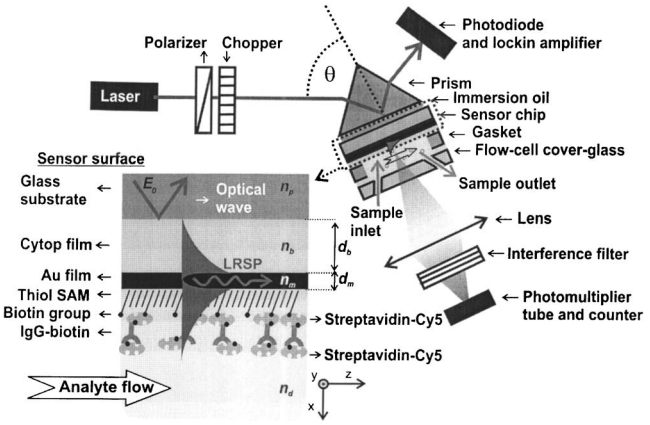

FIG. 1. Layer structure and optical setup for the excitation of LRSPs and its implementation for SPR and SPFS biosensing.

device was equipped with four equally spaced (1 mm) probes and was purchased from Keithley (Cleveland, OH). The two outer probes are used for sourcing current and the other two inner probes are used for measuring the resulting voltage drop across the surface of the sample. The volume resistivity is calculated as $\rho=\pi(\ln 2)^{-1}VI^{-1}d_m$, where ρ is volume resistivity (Ω cm), V is the measured voltage, I is the source current, and d_m is the gold layer thickness.

D. Optical setup for the excitation of long range surface plasmons

In this study, we used an optical setup based on the attenuated total reflection method with angular modulation of SPR described previously in more detail.[12] As shown in Fig. 1, a monochromatic light beam from a He–Ne laser emitting at a wavelength of $\lambda=632.8$ nm (PL610P, Polytec, Germany, power of 2 mW) or at a wavelength of $\lambda=543.5$ nm (LK54010P, Laser Graphics, Germany, power of 5 mW) was linearly polarized using a polarizer, passed through a chopper (Princeton Applied Research, TN), and was coupled to a 90° LASFN9 glass prism. Onto the prism base, a glass slide with a layer structure supporting LRSPs (Cytop layer coated by a gold film with a thickness of $d_m=14.6$ nm) or regular SPs (gold film with the thickness of $d_m=45$ nm) was optically matched using immersion oil (Cargile, NJ). The intensity of the light beam reflected at the prism base was measured using a photodiode and a lock-in amplifier (model 5210, Princeton Applied Research, TN). The angle of incidence of the light beam was controlled by using a rotation stage (Hans Huber AG, Germany) and the angular scans of the intensity of reflected light were measured as a function of the external angle of incidence θ. A flow-cell consisting of a poly(dimethylsiloxane) gasket and a glass support with drilled input and output ports (volume approximately 25 μl) was attached to the sensor surface to contain liquid samples. The input and output ports of the flow-cell were connected to a peristaltic pump (Reglo, Ismatec, Switzerland) using rubber tubing (Tygoon R3607, from Ismatec, Switzerland) in order to flow the liquid sample along the sensor surface (a flow rate of 500 μl min^{-1} was used). The fluorescence light emitted from

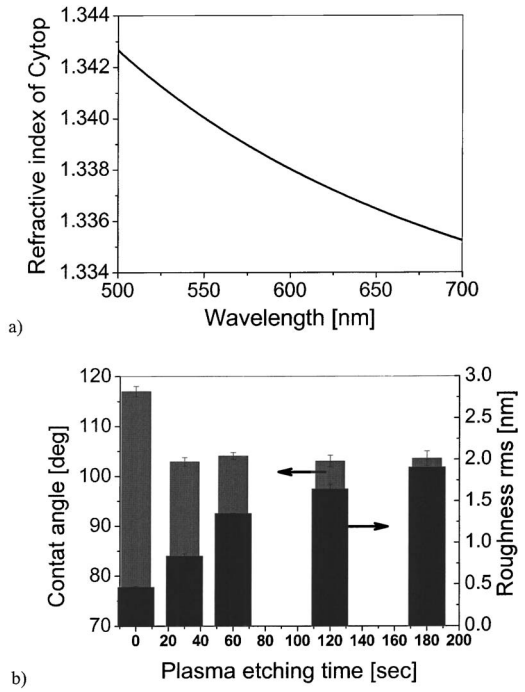

FIG. 2. (a) Refractive index dispersion n_b and (b) the dependence of contact angle and roughness on the O_2 plasma etching time of Cytop polymer.

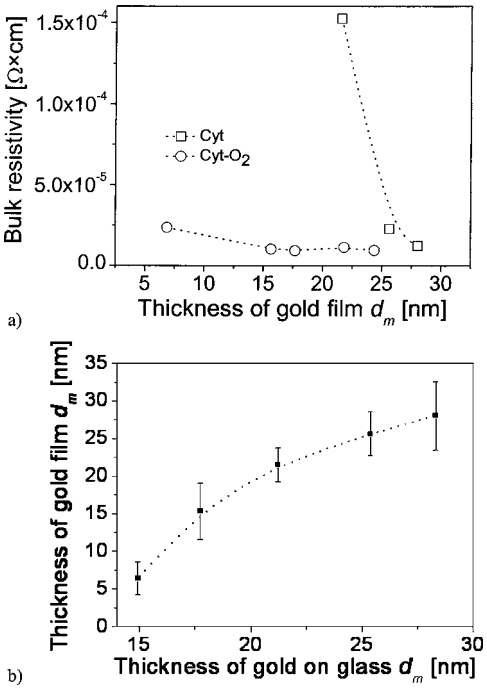

FIG. 3. (a) Thickness dependence of the bulk resistivity of gold film deposited on Cytop surface etched with O_2 plasma (Cyt-O_2) and not etched with O_2 plasma (Cyt). (b) The difference of the thickness of gold film d_m deposited by using thermal evaporation on a LASFN9 glass and on Cyt-O_2 surface.

chromophore-labeled molecules bound to the sensor surface was collected through the flow cell by using a lens; the light at the excitation wavelength was blocked by a bandpass filter (670FS10-25, L.O.T.-Oriel, Germany) and the intensity of fluorescence light was detected by a photomultiplier tube (H6240-01, Hamamatsu, Japan) that was connected to a counter (53131A, Agilent, CA). The control of the optical setup and the data collection were performed by using the software WASPLAS developed at the Max Planck Institute for Polymer Research in Mainz, Germany.

Measured reflectivity spectra were fitted with transfer matrix-based model[21] implemented in WINSPALL software developed at the Max Planck Institute for Polymer Research in Mainz, Germany. The enhancement of the electromagnetic field upon the excitation of surface plasmon modes was calculated by using a transfer matrix-based algorithm written in MAPLE (Waterloo Maple Inc., Canada).

III. RESULTS AND DISCUSSION

A. Characterization of multilayer structure

The refractive index of a Cytop layer was measured by ellipsometry at wavelengths between $\lambda=500$ and $\lambda=700$ nm. The obtained data presented in Fig. 2(a) reveal that Cytop exhibits the refractive index of $n_b=1.340$ and $n_b=1.337$ at the wavelengths of $\lambda=543.5$ nm and $\lambda=632.8$ nm, respectively. In general, fluoropolymers exhibit a low surface energy, which complicates their coating or bonding. In order to increase their surface energy, plasma or chemical etching was used.[22] As seen in Fig. 2(b), exposing the Cytop layer to O_2 plasma etching for 30 s resulted in an increase in the surface energy which is manifested as a decrease in the contact angle from 117.0° to 102.9°. Further increasing the O_2 plasma etching time did not change the contact angle significantly but the AFM characterization revealed that the root means square (rms) roughness σ of the Cytop surface gradually increased with the plasma etching time. For instance, 30 s O_2 plasma etching caused an increase in the rms roughness from 0.47 to 0.84 nm. In further experiments, we deposited gold films on Cytop surface not etched with plasma (abbreviated as Cyt), on the Cytop surface that was exposed to plasma etching for 30 s (abbreviated as Cyt-O_2) and directly on LASFN9 glass. The rms roughness of the gold film with the thickness of $d_m=14.6$ nm deposited on Cyt-O_2 surface ($\sigma=1.1$ nm) was approximately 2.5-fold lower than that observed on the Cyt surface ($\sigma=2.8$ nm) and it was comparable to the roughness of 45 nm thick gold film deposited on a polished LASFN9 glass slide ($\sigma=1.0$ nm).

Figure 3(a) shows the dependence of the resistivity of gold films deposited on Cyt-O_2 and Cyt surfaces on their thickness d_m. On the Cytop polymer not exposed to O_2 plasma etching, the coalescence transition was observed at a thickness of roughly $d_m=20$ nm. In contrast to that, the resistivity below 3×10^{-5} Ω cm was observed for gold films prepared on plasma-etched Cytop with the thickness down to $d_m=7$ nm. These data indicate that more compact gold films can be prepared on a Cyt-O_2 surface than on a pristine Cyt surface. In addition, let us note that the adhesion strength of gold film to the Cytop polymer on Cyt-O_2 surface was greatly increased compared to that on Cyt surface as tested

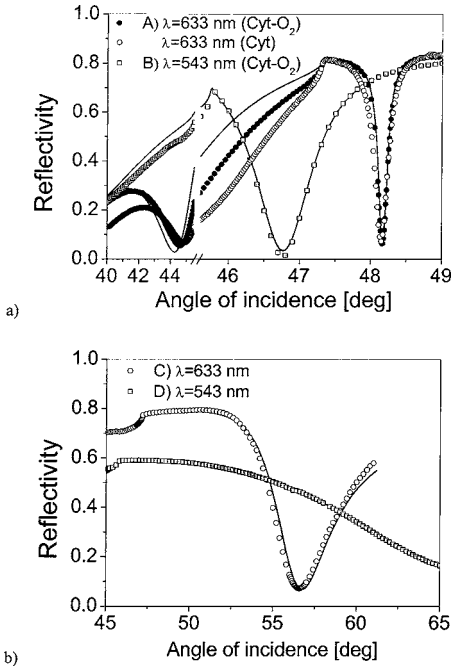

FIG. 4. (a) Reflectivity spectra for the excitation of LRSPs on a gold film with the thickness of d_m=14.6 nm deposited on Cyt-O_2 and Cyt surfaces. (b) Reflectivity spectra for the excitation of regular SPs on a 45 nm thick gold deposited on LASFN9 glass surface. The spectra were measured at the wavelengths of λ=543.5 (squares) and λ=632.8 nm (circles) and fitted with a transfer matrix-based model (lines).

by the "scotch tape test." Figure 3(b) shows the comparison of the thickness of gold films d_m deposited under identical conditions on Cyt-O_2 and glass surfaces. It reveals that the thickness measured on the Cytop surface is lower than the one on glass. The reason for this observation is probably due to the lower surface density of clusters from which the layer starts to grow on the Cytop surface.

B. Excitation of long range surface plasmons

We used a layer structure comprising a gold film with a thickness of d_m=14.6 nm sandwiched between water and the Cytop layer on the top of a glass substrate for the excitation of LRSPs. In order to achieve full coupling to LRSPs, the thickness of the Cytop buffer layer was adjusted to d_b =1150 nm for a wavelength λ=632.8 nm and to d_b =521 nm for a wavelength λ=543.5 nm. As Fig. 4(a) shows, the measured angular reflectivity spectra exhibit a dip associated with the resonant excitation of LRSPs centered at the angles of incidence θ=48.2° and 46.7° for the wavelength λ=632.8 and 543.5 nm, respectively. For the gold film on Cyt-O_2, the full width at half minimum (FWHM) of the LRSP resonance of $\Delta\theta$=0.18° and $\Delta\theta$=0.9° were measured at the wavelengths λ=632.8 nm and λ=543.5 nm, respectively. The LRSP resonance width $\Delta\theta$ for the Cyt-O_2 structure was of about 20% lower compared to that on the Cyt structure. Moreover, the excitation of regular SP on a structure with a gold film deposited on glass substrate with the thickness of d_m=45 nm is presented in Fig. 4(b). The coupling to SPs is manifested as resonant dip centered at a higher angles of incidence and with an order of magnitude larger FWHM compared to that for LRSPs. FWHM of $\Delta\theta$ =4.1° at a wavelength of λ=632.8 nm and $\Delta\theta$>10° at the wavelength λ=543.5 nm were observed for the excitation of SPs.

The measured reflectivity spectra in Figs. 4(a) and 4(b) were fitted by using the method of least squares and transfer matrix-based model in order to determine the optical properties of gold films.[21] In this analysis, we approximated the gold film as a homogeneous slab with an (effective) refractive index n_m and a thickness d_m that was measured by a surface profiler. The refractive index n_b and thickness d_b of Cytop layer, and the refractive index of water n_d and LASFN9 glass substrate n_p were determined by other methods or taken from literature as summarized in the Table I.

TABLE I. Parameters of layer structures and characteristics of LRSPs (A and B) and regular SPs (C and D) excited at wavelengths λ=632.8 and 543.5 nm.

Sample	Wavelength (nm)	Substrate and superstrate	Buffer layer	Gold film	Resonance FWHM (deg)	$\|\mathbf{E}\|^2/\|\mathbf{E}_0\|^2$
A	λ=632.8	n_p=1.845 n_d=1.333[a]	n_b=1.337 d_b=1150 nm	Re{n_m}=0.31±0.07 Im{n_m}=2.9±0.3 d_m=14.6±0.5 nm	$\Delta\theta$=0.18	88
B	λ=543.5	n_p=1.875 n_d=1.335[a]	n_b=1.340 d_b=521 nm	Re{n_m}=0.66±0.05 Im{n_m}=2.4±0.2 d_m=14.6±0.5 nm	$\Delta\theta$=0.9	19
C	λ=632.8	n_p=1.845 n_d=1.333[a]	···	Re{n_m}=0.124±0.002 Im{n_m}=3.561±0.002 d_m=45±1 nm	$\Delta\theta$=4.1	43
D	λ=543.5	n_p=1.875 n_d=1.335[a]	···	Re{n_m}=0.41±0.01 Im{n_m}=2.32±0.03 d_m=45±1 nm	$\Delta\theta$>10	6.3

[a]Reference 27.

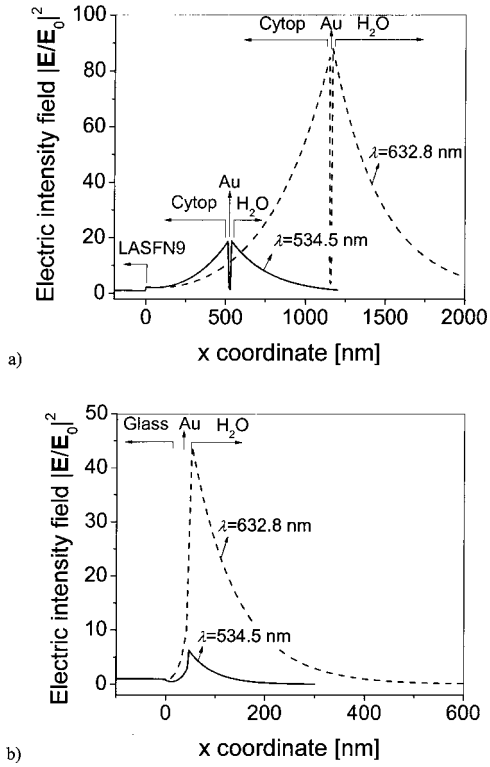

FIG. 5. Simulations of profile of electric intensity field upon the resonant coupling to (a) LRSP and (b) SP at wavelengths of λ=543.5 (solid line) and λ=632.8 nm (dashed line) calculated for the layer parameters in Table I.

The refractive index of a gold film deposited with the thickness of d_m=45 nm was fitted as n_m=0.12+3.561i for the wavelength λ=632.8 nm and as n_m=0.41+2.32i for the wavelength λ=543.5 nm. These values lie within the range reported in the literature.[23–25] For 14.6 nm thick gold film on Cyt-O_2 surface, the refractive indices of n_m=0.31+2.9i and n_m=0.66+2.4i were determined at a wavelengths of λ=632.8 nm and λ=543.5 nm, respectively. These data show that a thinner gold film on Cyt-O_2 surface exhibits changed real part of the refractive index Re{n_m} and a decreased imaginary part of the refractive index Im{n_m} which can be ascribed to the morphology changes. Let us note that the reflectivity spectrum for gold film deposited on Cytop surface without plasma etching (Cyt) was not possible to fit under the aforementioned approximations. Based on the determined parameters of the layer structures stated in Table I, we calculated the electric intensity field enhancement at the gold surface upon the resonant coupling to LRSPs and regular SPs. These simulations presented in Fig. 5 show that the excitation of LRSPs at the wavelength λ=632.8 nm provides larger enhancement of the electric intensity field in the vicinity to the gold surface ($|E|^2/|E_0|^2$=88) compared to that at the wavelength of λ=543.5 nm ($|E|^2/|E_0|^2$=19) for which the Ohmic losses in the gold are higher. As LRSPs propagate with lower damping than regular SPs, their excitation on the metallic surface provides stronger enhancement of electromagnetic field. In comparison to the excitation of regular SPs, the coupling to LRSPs on the prepared structures provides approximately two- and threefold increased enhancement of electric intensity field at the wavelength λ=632.8 nm and λ=543.5 nm, respectively. Let us note that the changes in the Re{n_m} and the decrease in the Im{n_m} of gold films prepared with the thickness of d_m=14.6 nm on Cytop shortens the propagation length of LRSPs and thus reduces the enhancement of electromagnetic field intensity. For instance, the simulations predict that at the wavelength of λ=632.8 nm, the excitation of LRSPs is accompanied with the enhancement of electric intensity field $|E|^2/|E_0|^2$=282 assuming a Cytop layer (d_b=1390 nm) and gold film (d_m=14.6 nm) with the refractive index identical to that for the 45 nm thick gold layer (n_m=0.12+3.561i). This field intensity enhancement is approximately threefold higher than that for the prepared gold film of which refractive index was determined as n_m=0.31+2.9i.

C. SPR and SPFS observation of affinity binding

The prepared layer structures for the excitation of LRSPs were employed for the observation of affinity binding of protein molecules on a gold sensor surface by using combined measurement of refractive index variations (SPR) and emitted fluorescence light (SPFS). We used a He–Ne laser with a wavelength of λ=632.8 nm and a layer structure supporting LRSPs with Cytop surface that was etched with plasma (Cyt-O_2) and that was not etched (Cyt) prior to the deposition of gold film (see parameters in Table I). For comparison, a layer structure supporting regular SPs on a 45 nm thick gold film was used. As depicted in Fig. 1, samples with the studied layer structures that were modified with mixed thiol SAM were optically matched to the prism base. First, PBS buffer was flowed across the sensor surface in order to establish a baseline. Afterwards, protein layers were grown on the surface during a successive flow of streptavidin (SA), biotinylated antibody (IgG), and SA dissolved at a concentration of 10 μg mL^{-1} in PBS buffer. Each solution with protein molecules was circulated through the flow-cell for 30 min followed by 10 min rising and measurement of angular fluorescence and reflectivity spectra.

Figure 6 shows the angular scans of the reflected and fluorescence light intensity measured after the successive binding of SA, IgG, and SA layers on a gold surface with thiol SAM biotin moieties. Figure 6(a) reveals that upon the binding of protein layers on the gold film deposited on Cyt-O_2 surface, the dip in the reflectivity spectrum due to the resonant excitation of LRSP shifts to the higher angles of incidence. After the binding of streptavidin labeled with Cy-5 chromophore, strong peak in the fluorescence spectrum rises at the angles of incidence for which the excitation of LRSP provides strongest enhancement of electromagnetic field. Similarly, Fig. 6(b) shows the changes in the reflectivity and fluorescence intensity spectra upon the assembly of protein layers on the 45 nm thick gold film probed with regular SPs. By fitting the measured reflectivity spectra and by assuming that the refractive index n on the sensor surface changes with the protein concentration c as $\partial n/\partial c \approx 0.17$ μL mg^{-1},[26] we calculated the surface coverage Γ of protein layers adhered to the metallic surface as summarized

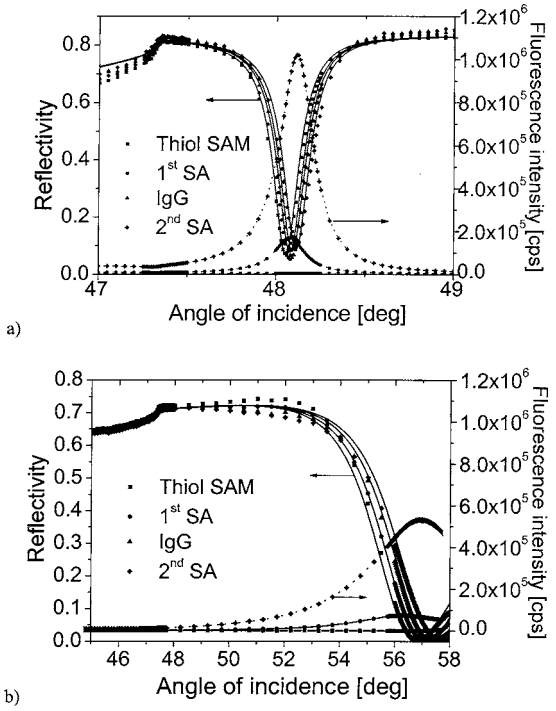

FIG. 6. (a) Angular reflectivity and fluorescence spectra measured upon the growth of SA and IgG protein layers for the excitation of (a) LRSPs (14.6 nm thick gold film on Cyt-O_2) and (b) regular SPs (45 nm thick gold film on LASFN9 glass) at the wavelength of $\lambda = 632.8$ nm

in Table II. These results show that the first and second streptavidin layers were immobilized with the surface coverage in the range $\Gamma = 1-2$ ng/mm^2 that is comparable with previously published results.[20] Probably owing to the more compact thiol SAM on a gold surface with lower roughness, approximately 20% larger surface coverage Γ of SA layers was observed on the 45 nm thick gold film compared to that on the 14.6 nm thick gold film. Due to the higher enhancement of electric field intensity, 2.1- and 1.8-fold stronger peak fluorescence signal was observed upon the probing the first- and second streptavidin layer, respectively, by LRSPs on 14.6 nm gold film attached to Cyt-O_2 surface (16.5×10^4 and 82.5×10^4 counts/s respectively) compared to that probed with regular surface plasmons on 45 nm thick gold film (8.1×10^4 and 45×10^4 counts/s, respectively). The fluorescence signal from the second SA film is approximately fivefold higher compared to that from the first SA layer owing to the decreased fluorescence quenching by Förster energy transfer.[16] The angular scans of the fluorescence intensity measured after the 30 min flow of a streptavidin solution across the thiol SAM without biotin moieties revealed that the peak fluorescence signal increased due to the nonspecific sorption to the surface of 0.3×10^4 and 0.9×10^4 counts/s for the probing with regular SPs and LRSPs, respectively. The sensor surface supporting the excitation of regular SPs showed smaller nonspecific signal because of the lower enhancement of electromagnetic field intensity and lower nonspecific sorption on the SAM with lower amount of defects. In addition, prior to the affinity binding of protein layers, the background signal was measured. Higher fluorescence signal of 3.6×10^4 was observed for the excitation of LRSPs compared to 0.8×10^4 counts/s observed for the excitation of regular SPs. The reason for this observation is probably due to the higher scattering on rougher surface and higher intensity of the autofluorescence light emitted transmitted from the prism through the thinner metallic film supporting LRSPs.

The time kinetics of the reflectivity and fluorescence signal were measured at an angle of incidence fixed to $\theta = 48.02°$, 48.08°, and 56.02° for the excitation of LRSPs on a gold film deposited on Cyt-O_2 and Cyt surface and for the excitation of regular SPs, respectively. Figure 7(a) shows the time evolution of the fluorescence signal and surface coverage Γ during the successive grow of SA, IgG, and SA layer on the sensor surface. In addition, Fig. 7(b) compares in detail the reflectivity and fluorescence signal kinetics upon the growth of the first SA layer on the thiol SAM with biotin moieties on the 14.6 nm thick gold films deposited on Cyt and Cyt-O_2 surface and on the 45 nm thick gold film deposited on glass. On all surfaces, the fluorescence signal increases due to the binding of SA labeled with Cy5 chromophore and it saturates after 3 min. However, the time evolution of reflectivity changes reveals that on smoother 45 nm thick gold film on glass, the response saturates faster (approximately after 3 min) compared to that on rougher 14.6 nm thick gold film on Cyt surface (more than 30 min).

TABLE II. Summary of surface characteristics and SPFS biosensor performance for protein layers grown on a thiol SAM-modified metallic film deposited on Cyt-O_2, Cyt, and glass.

	LRSP (Au/Cyt-O_2/glass)	LRSP (Au/Cyt/glass)	SP (Au/glass)
Gold surface rms roughness (nm)	1.1	2.8	1.0
First SA layer: Γ (ng mm^{-2})	1.3	···	1.6
IgG layer: Γ (ng mm^{-2})	0.7	···	1.7
Second SA layer: Γ (ng mm^{-2})	1.1	···	1.3
First SA layer: F (10^4 counts/s)	16.9	12.3	8.1
Second SA layer: F (10^4 counts/s)	82.5	32.6	45
None-specific binding: F (10^4 counts/s)	0.9	1.3	0.3
Background: F (10^4 counts/s)	3.6	2.8	0.8

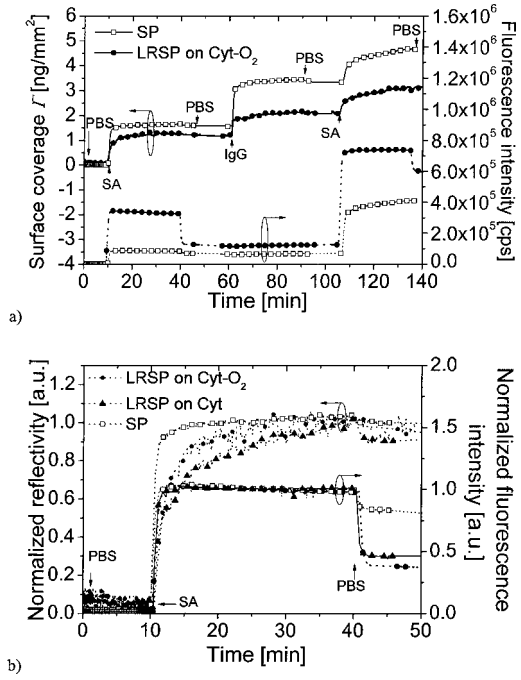

FIG. 7. (a) Time evolution of protein surface coverage and fluorescence signal measured for a successive growth of SA, IgG, and SA layers probed by LRSPs (14.6 nm thick gold film on Cyt-O_2) and regular SPs (45 nm thick gold film on glass). (b) Detail of the time evolution of the reflectivity and fluorescence signal measured upon the affinity binding of first SA layer on the surface with 14.6 nm thick gold film deposited on Cyt and Cyt-O_2 (probing by LRSPs) and on 45 nm thick gold film deposited on glass (probing by regular SPs).

The reason for this observation is probably that two binding mechanisms are superimposed. The fast changes in the sensor signal within 3 min after the sample injection is probably due to the affinity binding of SA to biotin moieties in the surface. The slower response can be attributed to nonspecific binding on a surface due to the defects in the thiol SAM that are more pronounced on rougher surfaces. The fact that this binding mechanism does not change the fluorescence signal indicates that the binding probably occurs directly on the gold surface where it is strongly quenched.

IV. SUMMARY

We examined the characteristics of thin gold films deposited by thermal evaporation on Cytop fluoropolymer layer and investigated how they affect the performance of biosensors based on SPR and SPFS employing the excitation of LRSPs. We observed that the roughness of gold films deposited on Cytop is higher compared to that for gold films deposited on glass due to the low surface energy of Cytop fluoropolymer. The increasing surface energy of Cytop by etching with O_2 plasma allowed the preparation of smoother and more compact gold films. The prepared layer structures were used for the SPR and SPFS-based observation of affinity binding of protein molecules to the sensor surface that was modified by mixed thiol SAM. The results revealed that the gold roughness affects the binding capacity and nonspecific interactions of protein molecules with the surface. By using the prepared structures for excitation of LRSPs, approximately twofold increased enhancement of electric intensity field and fluorescence signal in close proximity to the surface was observed with respect to conventional SPFS. The simulations predict that further improving the quality of gold films on Cytop surfaces would allow for additional threefold increase in the enhancement of electric intensity field through the excitation of LRSP on a surface of studied SPFS biosensor.

ACKNOWLEDGMENT

The authors would like to thank Andreas Unger from Max Planck Institute for Polymer Research in Mainz, Germany, for the characterization of the Cytop films by means of ellipsometry.

[1]D. Sarid, Phys. Rev. Lett. **47**, 1927 (1981).
[2]A. Boltasseva, T. Nikolajsen, K. Leosson, K. Kjaer, M. S. Larsen, and S. I. Bozhevolnyi, J. Lightwave Technol. **23**, 413 (2005).
[3]R. Charbonneau, C. Scales, I. Breukelaar, S. Fafard, N. Lahoud, G. Mattiussi, and P. Berini, J. Lightwave Technol. **24**, 477 (2006).
[4]H. J. Simon, Y. Wang, L. B. Zhou, and Z. Chen, Opt. Lett. **17**, 1268 (1992).
[5]T. Okamoto, J. Simonen, and S. Kawata, Phys. Rev. B **77**, 115425 (2008).
[6]G. Winter, S. Wedge, and W. L. Barnes, New J. Phys. **8**, 125 (2006).
[7]T. Inagaki, M. Motosuga, E. T. Arakawa, and J. P. Goudonnet, Phys. Rev. B **32**, 6238 (1985).
[8]J. Dostálek, R. F. Roskamp, and W. Knoll, Sens. Actuators B **139**, 9 (2009).
[9]K. Matsubara, S. Kawata, and S. Minami, Opt. Lett. **15**, 75 (1990).
[10]G. G. Nenninger, P. Tobiska, J. Homola, and S. S. Yee, Sens. Actuators B **74**, 145 (2001).
[11]A. Kasry and W. Knoll, Appl. Phys. Lett. **89**, 101106 (2006).
[12]J. Dostalek, A. Kasry, and W. Knoll, J. Comput.-Aided Des. Comput. Graphics **2**, 97 (2007).
[13]S. Slavik and J. Homola, Sens. Actuators B **123**, 10 (2007).
[14]A. W. Wark, H. J. Lee, and R. M. Corn, Anal. Chem. **77**, 3904 (2005).
[15]J. Dostalek and W. Knoll, BioInterphases **3**, FD12 (2008).
[16]T. Liebermann and W. Knoll, Colloids Surf., A **171**, 115 (2000).
[17]P. D. Keathley and J. T. Hastings, J. Vac. Sci. Technol. B **26**, 2473 (2008).
[18]M. Vala, J. Dostalek, and J. Homola, Proc. SPIE **6585**, 658522 (2007).
[19]E. M. Liston, L. Martinu, and M. R. Wertheimer, J. Adhes. Sci. Technol. **7**, 1091 (1993).
[20]W. Knoll, M. Zizlsperger, T. Liebermann, S. Arnold, A. Badia, M. Liley, D. Piscevic, F. J. Schmitt, and J. Spinke, Colloids Surf., A **161**, 115 (2000).
[21]P. Yeh, *Optical waves in Layered Media* (Wiley, New York, 1998).
[22]S. R. Kim, J. Appl. Polym. Sci. **77**, 1913 (2000).
[23]M. A. Ordal, L. L. Long, R. J. Bell, S. E. Bell, R. R. Bell, R. W. Alexander, and C. A. Ward, Appl. Opt. **22**, 1099 (1983).
[24]E. D. Palik, *Handbook of Optical Constants of Solids* (Academic, New York, 1985).
[25]A. Rueda, N. Vogel, and M. Kreiter, Surf. Sci. **603**, 491 (2009).
[26]B. Liedberg, I. Lundstrom, and E. Stenberg, Sens. Actuators B **11**, 63 (1993).
[27]G. M. Hale and M. R. Querry, Appl. Opt. **12**, 555 (1973).